Journal of Agricultural Science; Vol. 8, No. 9; 2016
ISSN 1916-9752 E-ISSN 1916-9760
Published by Canadian Center of Science and Education

Soil Mapping in Chongwe, Zambia by Digital Analysis of Landsat Data

Chizumba Shepande[1], Marvin Bauer[2], Jay Bell[2] & Victor Shitumbanuma[1]

[1] School of Agricultural Scinces, Department of Soil Science, Universityof Zambia, Lusaka, Zambia

[2] College of Food, Agriculture and Natural Sciences, University of Minnesota, St Paul, Minnesota, USA

Correspondence: Chizumba Shepande, School of Agricultural Sciences, Department of Soil Science, University of Zambia, Lusaka, Zambia, P.O. Box 32379, 10101 Lusaka, Zambia. Tel: 260-975-443-485. E-mail: shepande@yahoo.com

Received: March 4, 2016 Accepted: July 4, 2016 Online Published: August 15, 2016

doi:10.5539/jas.v8n9p152 URL: http://dx.doi.org/10.5539/jas.v8n9p152

Abstract

Designing a methodology for mapping and studying soils in a quick and inexpensive way is critical especially in developing countries like Zambia, which lack detailed soil surveys. Therefore, this study was conducted to determine the potential of Landsat 7 ETM+ data (Enhanced Thematic Mapper plus) in mapping soils in Chongwe, a semi-arid region in Zambia. In addition, the study attempted to establish how accurate spectral soil maps produced by digital analysis of Landsat data can be and how such maps compared with field observation data. Also, in situations where there was poor agreement between Landsat data and field observation data, possible causes of such discrepancies where determined.

A soil inventory of the Chongwe region of Zambia was prepared using computer-aided digital analysis of two Landsat 7 ETM+ satellite images acquired in the dry and rainy seasons to investigate the hypothesis that there is a relationship between Landsat spectral reflectance and certain soil types and that this relationship can be used to map soils with reasonable accuracy.

The study revealed that digital analysis of Landsat 7 ETM images has the capacity to map and delineate soil patterns with reasonable accuracy, especially when acquired during the dry season when there are long periods of cloud free skies, low soil moisture and minimal vegetation cover. The overall agreement between the Landsat classification and reference data was 72%, indicating a definite relationship between Landsat imagery and soil types.

In terms of soilscape boundary delineation, the Landsat derived map was had a higher level of agreement with field observations than the conventional soil map. In addition, the study showed that overall, upland areas have a better agreement with Landsat spectral data compared to lowland areas, probably due to the diverse origin of sediments and low spatial extent of most landforms in lowland areas.

Keywords: soil mapping, landforms, remote sensing, image classification, spectral class, classification accuracy

1. Introduction

Remote sensing techniques are continuously being evaluated to determine where they are appropriate and applicable. Weismiller, Persinger, and Montgomery (1977) reviewed the characteristics of Landsat data and concluded that these data are applicable to soil survey because of synoptic view, ability to collect temporal data, multispectral data collection and possible correlation of soil patterns with spectral characteristics. In a study on the reflectance of some typical soils of India, Dwivedi, Singh, and Raju (1981) concluded that different soils can be separated using spectral reflectance data. However, classification accuracy depends on the quality of the image acquired and on the methods of analysis used (Duggin & Robinove, 1990).

The use of Landsat data for soil mapping is typically by digital analysis of images or by visual interpretation of false color composites. Reddy and Hilwig (1993), and Buiten (1993) favor the digital approach of image interpretation because it is quantitative and applies automated classification methods, pixel by pixel. This is confirmed by earlier work conducted by Zachary, Cipra, Diderickson, Kristof, and Baumgardner (1972), who used remotely sensed data to study the soils of Indiana, and found that there was a definite relationship between multispectral imagery and soil types. This work also revealed that large areas of bare soil could be mapped rapidly by digital analysis, a technique that has been supported by Cipra, Baumgardner, Stoner & MacDonald

(1980), who observed a good agreement between Landsat spectral characteristics and soil properties from non-vegetated sites. Studies conducted earlier (Kristof & Zachary, 1971; Mathews, Cunningham, Cipra, & West, 1973; Westin & Frazee, 1976; Weismiller et al., 1979) also indicated that digital analysis of multispectral imagery could be successfully used in soil mapping. A study by Cohen and Goward (2003) also confirms the capability of Landsat in ecological applications of remote sensing.

In-spite of the wide-spread use of Landsat data for mapping natural resources, digital analysis of Landsat ETM+ data have not been studied or applied to soil survey in semi-arid Zambia resulting in lack of detailed soil surveys. Therefore, designing a methodology for mapping soils in a quick and inexpensive way would be beneficial for Zambia. The objectives of this research (Shepande, 2010) were to determine how spectral soil maps produced by digital analysis of Landsat ETM data compared with field observations in the Chongwe region of Zambia. In a further objective, where good agreement was not obtained between Landsat imagery spectral characteristics and field observation data, an attempt was made to determine why the discrepancies occurred.

2. Methods

2.1 Physical Setting

The study area, covering 54,000 ha is located about 45 km east of the capital city, Lusaka, Zambia. Geologically, the project area comprises Precambrian metasediments of the Basement complex made up of the gneiss group, a younger sequence of Rufunsa quartzite, schist and limestone (Brandt, 1958). Pleistocene to recent sediments include alluvium, calcareous tufa and laterite. According to Dixey (1955), physiographically, the area is mainly a peneplain geomorphic surface consisting of plateau, irregular piedmonts, outlier hills, dambo areas and an undulating river plain marked with paleochannels, terraces and overflow basins. The climate of the area is semi-arid with ustic soil moisture and hyperthemic soil temperature regimes. The vegetation is predominantly acacia, interspaced with isolated pockets of drought resistant shrubs. Except for wet dambo areas, most of the land is bare during the dry season.

2.2 Data Set Formulation

Clear and cloud-free Landsat 7 ETM + data were acquired on 17 January, 2009 and 9 July, 2009 for path 171 and row 71, an area covering the eastern part of Lusaka district where the project site is located. These data were utilized as the main data source for this study.

Soil profiles and auger holes were studied at selected locations in each geomorphic unit and described according to the FAO guidelines for soil profile description (FAO, 1990). A total of 53 soil profile pits and 89 auger holes were studied.

The portion of the scene containing the Chongwe region was selected for preprocessing. Landsat data collected on July 9, 2009 were rectified to UTM zone 35S, Clark 1880, Arc 1950 using 42 well defined, spatially small and evenly distributed ground control points selected from the Zambia Sheet 1528 B3 topographic map (1:50,000) covering the study area. The rectification process met the criteria for accuracy as the image was rectified with a root mean square error of 4.96, which is less than one quarter pixel of a 30-meter resolution image. The image was resampled using the nearest neighbor method to calculate the new pixel values. This procedure produced a data set of 1:50,000 scale and registered geographic points in the image data to their exact ground position. The January 17, 2009 image was registered to the rectified image using the Auto Sync operations in ERDAS Imagine Software.

Using the topographic map, other topographic features were digitized and overlaid on the Landsat data. These features included rivers and broad physiographic boundaries (valleys, plains and piedmonts). A-90 meter Shuttle Radar Topographic Mission (SRTM) digital elevation model produced by NASA and contour lines were downloaded and processed. A soil survey map (Figure 3) at 1:50,000 scale which covers a small portion in the middle part of the study area was also digitized and overlaid on the image. This soil map, produced by the Soil Survey Unit of the Department of Agriculture-Zambia (1988) covers a commercial pivot-irrigated farm area which was mapped and classified using traditional soil survey methods through visual interpretation of 1:50,000 scale aerial photographs. For this survey, soils were mapped using the World Reference Base for Soil Resources (ISRIC, 1989) and interpreted into the USDA Soil Taxonomy (USDA, 2003) at subgroup level.

2.3 Atmospheric Correction

The atmosphere affects the radiance received at the satellite by scattering, absorbing and refracting light (Dozier & Frew, 1981; Chavez, 1989; Moran et al., 1992). Corrections for these effects must be included in radiometric procedures that are used to convert satellite-recorded digital counts to ground reflectances. Different procedures

for atmospheric correction have been proposed for digital data in the visible and near-infrared (Otterman & Fraser, 1976; Dozier & Frew, 1981; Sing, 1988; Piwowar & LeDrew, 2001).

In this study, atmospheric and radiometric correction of Landsat 7 ETM data was done using the COST model of Chavez (1996). This image-based technique for atmospheric correction uses scene dependant inputs to obtain the necessary model constants, after which raw DN are easily converted to atmospherically corrected reflectance values. The scene dependent inputs required for this model to run are: solar radiation angle, data of image acquisition, earth-sun distance and minimum DN values for each band.

2.4 Image Classification

The first step of image classification involved a generalized unsupervised classification using bands 3, 5 and 7 to segment the image data into 21 clusters of different spectral radiometric classes. The classes were later merged after field observation since in some cases, one soil unit was represented by two or more spectral classes. Field observation was performed through spot identification and image correlation, which was followed by soil unit delineation and soil profile description. While in the field, polygons were drawn on the hard copy image around some soil units that would help locate training pixels for supervised classification.

The unsupervised image with merged classes was used to create another image by supervised classification. This technique used samples of known identity to classify pixels of unknown identity. The supervised classification scheme with 13 classes was based on the geomorphic units identified in the study area and other local knowledge sources. Recognition of pixels in the unsupervised image that represented the soil units of interest was very useful in identifying training sites for each unit.

Training data were obtained by on-screen digitizing of polygons over the rectified raster image in ERDAS Imagine Software. Eight to ten polygons were digitized for each soil unit category to ensure sufficient and representative information to create the spectral signatures. Each training polygon constituted an area with multiple pixels. The soil units of interest are listed in Table 2. Ellipses of training data were examined on scatter plots of the image data to see if there were areas without training. Additional training was set up for such areas. The maximum likelihood classifier was used in assigning each pixel to its most likely class. Of the 142 sample polygons, 93 were used for training the classifier, and 49 were used for accuracy assessment. Post-classification filtering was done using a 3 × 3 majority filter in ERDAS Imagine to show only the dominant classification.

3. Results and Discussion

Viewing the 90-meter SRTM digital elevation model (DEM) and Landsat data together made it possible to examine the same soilscapes in both formats at the same time. Except for hilly areas, the DEM did not add significantly to the soilscape information extractable from the Landsat imagery. This is because the DEM was too coarse for this scale of mapping and was therefore not very helpful due to lack of sufficient detail. Other than a few outlier hills, the study area is mainly gently sloping to almost flat with the dominant slope being less than 4%.

Therefore, the topographic information added by the DEM was not of sufficient spatial resolution to clarify most of the soilscape boundaries. However, in isolated locations with steeper slopes as those in outlier hills in the southern part of the study area shown in Figure 1, the position of soilscape boundary was identifiable using the DEM. This indicates that the DEM is not helpful for landscapes that are generally flat, with very gentle slopes, but appear to be helpful in areas with high relief.

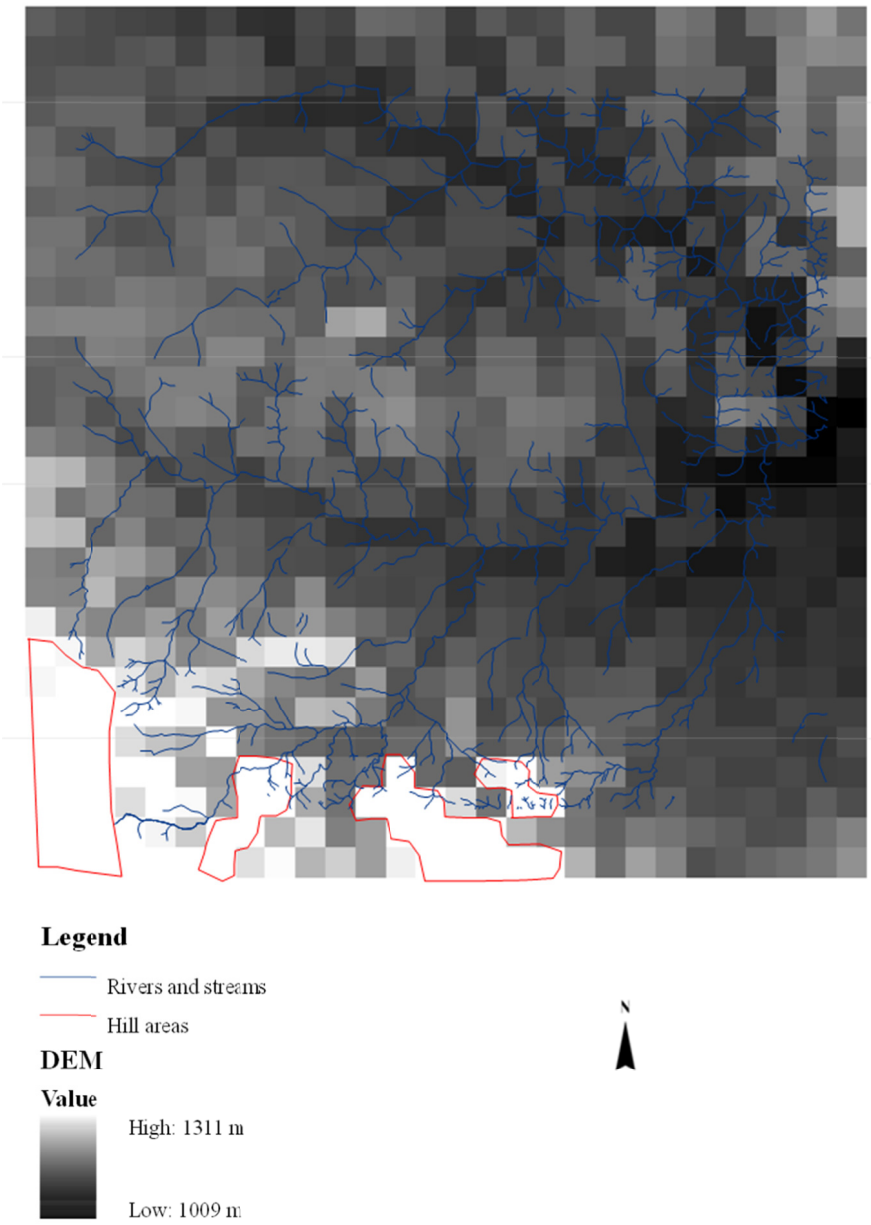

Figure 1. Identification of soilscape boundaries and hill land areas based on the digital elevation model (DEM) of the study area

The Landsat 7 ETM+ data were examined for the images representing different seasons. The January 17, 2009 image represents the beginning of the rainy season and the July 9, 2009 image represents the long dry season characterized with scarcity of vegetation and long periods of cloud-free skies. In January, vegetation was dormant due to the preceding long dry season and most of the pastures had been extensively grazed. The spectral responses for this image were not well related to ground reference information, mostly because response differences in vegetation were obscured by overgrazing and insignificant re-growth due to drought in the preceding season. In portions of the study area that were not overgrazed, the stress free vegetation was growing vigorously and the soil surface was masked by the uniform appearance of vigorous vegetation cover. The spectral properties of the soil were therefore not directly observable. In these areas, it was difficult to relate soil surface reflectance to soilscapes. Since pattern recognition was poor, data for the January image were not processed further.

The July image (representing features in the dry season) showed patterns similar to those observed on the ground. The false color composite of this image in bands 3, 5, and 7 visually revealed a better correspondence with the

soilscapes as shown in Figure 2. These results indicate that the best time for acquiring soil information via Landsat data from natural landscapes in semi-arid regions of Zambia is in the dry season. This is attributed to low soil moisture, long periods of cloud-free skies and minimal crop and vegetation cover (Zidat, Taylor, & Brewer, 2003).

There were 17 spectral classes in the supervised classification of the study area. The informational classes represented by the 17 spectral classes, their proportion, and the number of spectral classes in each information class are shown in Table 1. In vegetated portions of the study area, the spectral characteristics of the soil surface were not directly observable. In these circumstances vegetated portions that were not sampled during field work were assigned to the adjacent soil units, while those that were sampled were assigned to their respective soil classes. On this basis, the original 17 spectral classes where merged into 13 (Tables 3 and 4).

Table 1. Spectral classes derived from supervised classification of Landsat 7 ETM+ for the study area

Informational class	Number of spectral classes	Area coverage (%)
Bare soils	13	92
Vegetation (trees, shrubs, grass)	3	7
Water	1	<1

The 13 spectral classes presented in Tables 3 and 4 with their associated landform, drainage class and soil classification are relevant to pedology and are rational in the sense that they include areas that differ in landscape position, composition, age, as well as in natural soil drainage. It is worth noting that in most cases, there is not a direct one-to-one correspondence between soil subgroups and spectral classes. This was also evident when the soil observation points were plotted on the classified image. For example, in some cases one spectral class represents two or more soil subgroups, and in other cases a single soil subgroup is represented by one or more spectral classes. However, due to the use of sub-group level for classification and the use of landforms as mapping units many of the soil sub-groups within a spectral group are in close genetic relationship. Tables 3 and 4 show the correlation of spectral classes with individual soil sub-groups for the upland and lowland geomorphic units (landforms), respectively.

Landsat data mainly capture features on the surface of the earth, while the soil classification at sub-group level is mainly based on subsurface properties of the soil that cannot readily be captured by surface observations via Landsat imagery. It is therefore, not surprising that soils that are grouped within one class based on pedological features, may fall with different spectral reflectance on Landsat imagery, if the surface features of the soil differ.

Table 2. Physiographic description and soils of the study area

Relief type	Lithology	Spectral color (FCC:3,5,7)	Landform (Geomorphic unit)	Mapping unit code	Soil composition FAO	Soil composition Soil Taxonomy
Hilland						
Scarp	Hematite banded quartzite	Dark green	Scarp	Hl 1.1	Rhodic Ferrasols	Rhodic Haplustox
Outlier hills	Hematite banded quartzite	Dark green	Slope complex	Hl 1.2	Rhodic Ferrasols	Rhodic Haplustox
Piedmont						
Upper piedmont	Schist/quartzite	Dark purple	Upper piedmont	Pt 2.1	Plinthic & Rhodic Ferrasols	Plinthic Haplustox, Typic Haplustox, Rhodic Haplustox
Lower piedmont	Schist/gneiss	Purple	Lower piedmont	Pt 2.2	Ferric Acrisols & Haplic Arenosols	Typic Paleustults, Typic Rhodustults, Typic Dystrustepts
Plateau						
Plateau Summit	Gneiss	Very light green	Flat surfaces (crest)	Plt 3.1	Ferric Acrisols	Typic Paleustults, Typic haplustults
Upper plateau	Quartz/Mica Schist & dolomitic limestone	Whitish	Upper slope	Plt 3.2	Ferric Luvisols	Typic Paleustults, Typic Rhodustults
Lower plateau	Colluvial sands, dolomitic limestone	Whitish	Lower slope	Plt 3.3	Ferralic Arenosols	Ustic Quartzpsamments, AquicUstorthents
Plateau depression	Quartzite/Schist	Very light purple	Upland depression	Plt 3.4	Ferric Cambisols	Typic Endoaquepts, Typic Haplustepts, Aquic Haplustepts
Alluvial plain						
High terrace	Alluvium derived from schist	Light yellowish green	Tread/riser complex	RP 4.1	Umbric fluvisols	Typic Ustifluvents, Aquic Ustifluvents
Lower terrace	Recent alluvium	Light green	Riser	RP 4.2	Umbric fluvisols	Typic Ustifluvents, Typic Udifluvents
	Recent alluvium	Light green	Tread	RP 4.3	Chromic Luvisols	Typic Kandiustults, Rhodic Kandiustults
	Recent alluvium	Black	Overflow basin	RP 4.4	Chromic Vertisols	Typic Calciaquerts
Vale	alluvium	Green	Old river channel	RP 4.5	Vertic Luvisols	Vertic Endoaqualfs, Typic Ustifluvents
Valley dambo						
Narrow head	colluvial deposits over dambo alluvium	Black	Narrow depression	VD 5.1	Dystric Gleysols	Typic Fluvaquents
Broad head	colluvial deposits over dambo alluvium	Very dark brown	Broad depression	VD 5.2	Eutric Gleysols	Mollic Endoaqualfs

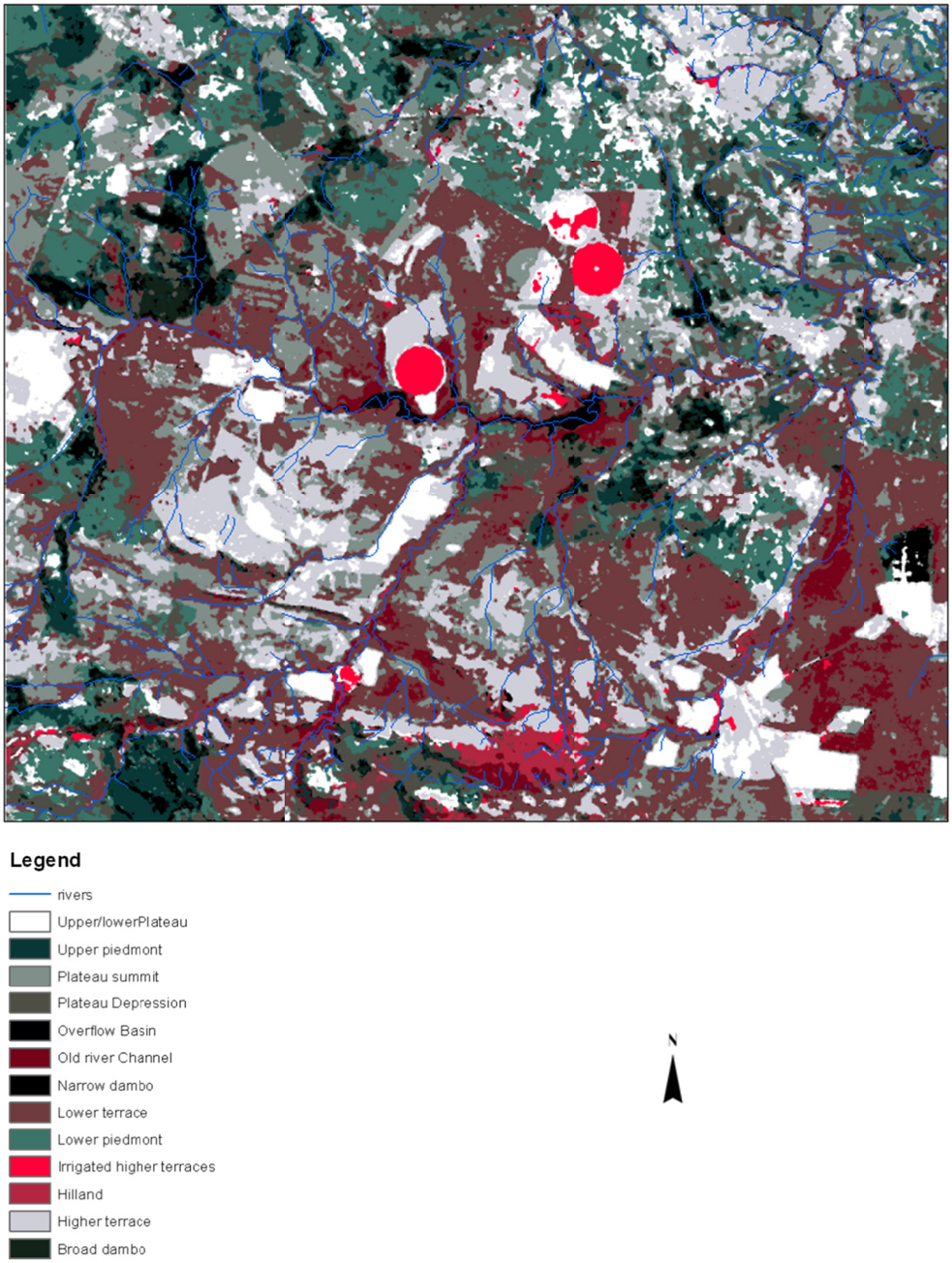

Figure 2. Landsat-derived geomorphic units in the study area prepared by supervised classification of the dry-season Landsat ETM+ data in bands 3, 5 and 7

Table 3. Association between spectral class, landform, drainage class and soil classification at sub-group level of up-land geomorphic units

Spectral class	Geomorphic unit (soilscape)	Subgroup classification	Soil drainage class
1	Hilland (outlier hills and scarps)	Rhodic Haplustox	Well drained
2	Upper piedmont	Typic Haplustox, Plinthic Haplustox	Well drained
3	Lower piedmont	Typic Rhodustults, Typic Dystrustepts	Well drained
4	Plateau summit	Typic Haplustults, Typic Paleustults	Well drained
5	Upper/lower plateau	Typic Paleustults, Ustic Quartzsamments	Well drained
6	Plateau depression	Aquic Haplustepts, Typic Haplustepts, Typic Endoaquepts	Medium drained

Table 4. Association between spectral class, landform, drainage class and soil classification at sub-group level of low-land geomorphic units

Spectral class	Geomorphic unit (soilscape)	Subgroup classification	Soil drainage class
7	Higher terrace	Aquic Ustifluvents	Well drained
8	Higher terraces (Irrigated)	Aquic Ustifluvents	Well drained
9	Lower terrace	Typic Udifluvents, Typic Ustifluvents,	Well drained
10	Overflow basin	Typic Calciaquerts	Poorly drained
11	Old river channel	Vertic Endoaqualfs, Typic Ustifluvents	Poorly drained
12	Narrow depression	Typic Fluvaquents	Poorly drained
13	Broad depression	Mollic Endoaquafs	Poorly drained

Although overall, there was good agreement between Landsat spectral data and field observations, some discrepancies occurred between the two sets of data. Field investigation identified 15 geomorphic units as shown in the physiographic description of the study area (Table 2) while the final supervised classification image has only 13 units (Tables 3 and 4). This can be attributed to the fact that related geomorphic units with similar spectral characteristics could not be spectrally separated; these were instead grouped and classified as one unit.

Soils developed on the quartzite upper plateau (Plt 3.2) were not differentiated spectrally from quartzite-derived colluvial sands of the lower plateau (Plt 3.3). Examination of field reference data indicated that the color of the topsoil in both units was yellowish red (5 YR4/6), which was the same color as that of the many termite mounds observed in both units (Figure 5). Over years these termite mounds are washed down and hence influencing the color of the surface soil in both units and demonstrating the influence of termite activities or bioturbation on soil color. In addition, colluvial material deposited from upper plateau areas onto the lower plateau enhances the similarity of soil color in these two units. It is clear from the spectral behavior of these two units that soil color had an overriding influence on their spectral characteristics. The predominant soil taxa in this unit is Typic Paleustults. Ustic quartzisamments occur as inclusions adjacent to the upper plateau.

As shown in Figure 2, the riser (Rp 4.2) and tread (Rp 4.3) landforms on recent alluvium were also spectrally inseparable probably due to similarities in depositional environments and characteristics of the alluvium. These two units occur adjacent to the Chongwe and Chalimbana rivers as well as their tributaries. Fluvial deposits from Chongwe and Chalimbana rivers are very common in both units. Field identification of these landforms was based on slope steepness (2-3% for riser and 0-1% for tread). Possible misinterpretation of slope data in some locations could lead to confusion in the identification of these two landforms. This could have been avoided if a high resolution digital elevation model was applied in the interpretation of these landforms. Field reference data showed that the topsoil in both units was reddish brown to brown due to the similar depositional environment and hence their similarities in spectral reflectance. The predominant soils in this unit were Typic Ustifluvents, although our field data indicated inclusions of Typic kandiustults, especially in areas adjacent to the higher terraces.

Quartzite scarps and outlier hills of the hill-land area were spectrally inseparable. Field data indicated that these landforms are both characterized by a general shallowness of soils to bedrock and high frequency of quartzite outcrops. In addition, both units bear characteristics of an erosion surface with a thin layer of reddish yellow (7.5

YR 7/6) sandy loams to loamy sands. As such these landforms were spectrally homogenous. No detailed soil profile examinations were made in these areas due to shallow depth to bedrock and many outcrops.

The Landsat image also recorded some features which do not relate to soil variability, for instance, center pivot irrigated farms which appear as reddish circular patterns are spectrally different from surrounding areas due to high absorption by soil moisture in the Landsat bands (Figure 2). These areas, that were mapped as irrigated higher terraces (spectral class 8, Table 4) on the Landsat derived map do not necessarily follow patterns of soil variation, but also land management. Field examination, which included detailed soil profile descriptions, revealed that soils in this mapping unit were morphologically similar to those in the higher terraces (spectral class 7, Table 4). Soils in these spectrally different but morphologically similar landforms (higher terraces and irrigated higher terraces) were found to be the same and were both classified as Aquic Ustifluvents.

When a digitized soil survey map covering a small portion in the middle of the project area was interfaced with the classified July 2009 image (Figure 4) most soil polygons matched the spectral patterns in the imagery. This indicates that some soil polygons in the soil survey map match reflectance values in the Landsat image. The Landsat ETM-derived soil map is presented in Figure 2 and the conventional soil survey map is shown in Figure 3. To determine the reliability of the soil map derived from Landsat ETM data, we compared it with the conventional soil survey map which was prepared by the Soil Survey Unit of the Department of Agriculture-Zambia (1988). This map was made through systematic visual interpretation of 1:50,000 scale aerial photographs. It is seen from the conventional soil survey map that the boundaries of polygons A, B, C, F, L, and Q are mapped similar to the Landsat derived soil map (Figure 4) and that they correspond, respectively, to the higher terrace, plateau summit, lower terrace, overflow basin, and upper/lower plateau on the Landsat-derived soil map.

Polygon T in the south west corner of the conventional soil survey map was also mapped similar to the Landsat derived-derived soil map. The only discrepancy is that on the conventional soil map this area is mapped as Acquic Ustifluvents (Figure 3), whereas on the Landsat-based map, it was mapped as Typic Ustifluvents. Polygon S on the conventional map corresponds to the overflow basin on the Landsat soil map. However, its areal extent on the Landsat map is comparatively less as part of it is mapped as an old river channel (Paleochannel).

With respect to delineation of boundaries, the Landsat derived soil map in some cases differed from the conventional soil map. For example, two geomorphic units (overflow basin and old river channel) were mapped within the one unit of the conventional soil map. The conventional soil map did not separate the two units probably due to similar depositional environment in the overflow basin and the old river channel.

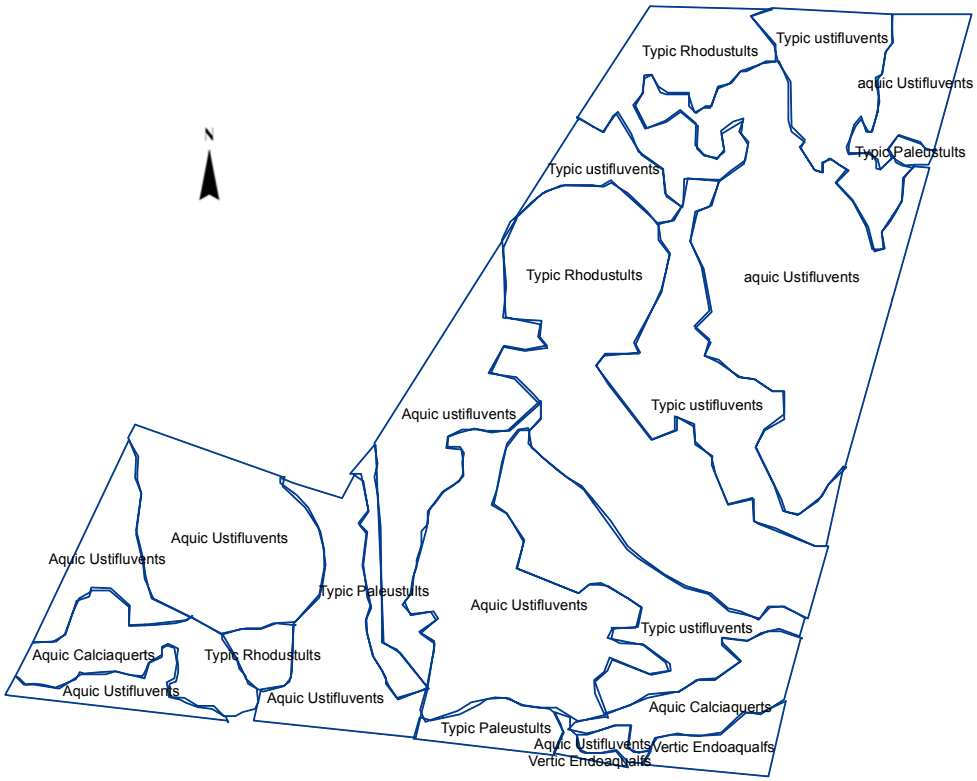

Figure 3. Digitized conventional soil survey map covering a portion of the study area.

Note. Scale: 1:50,000.

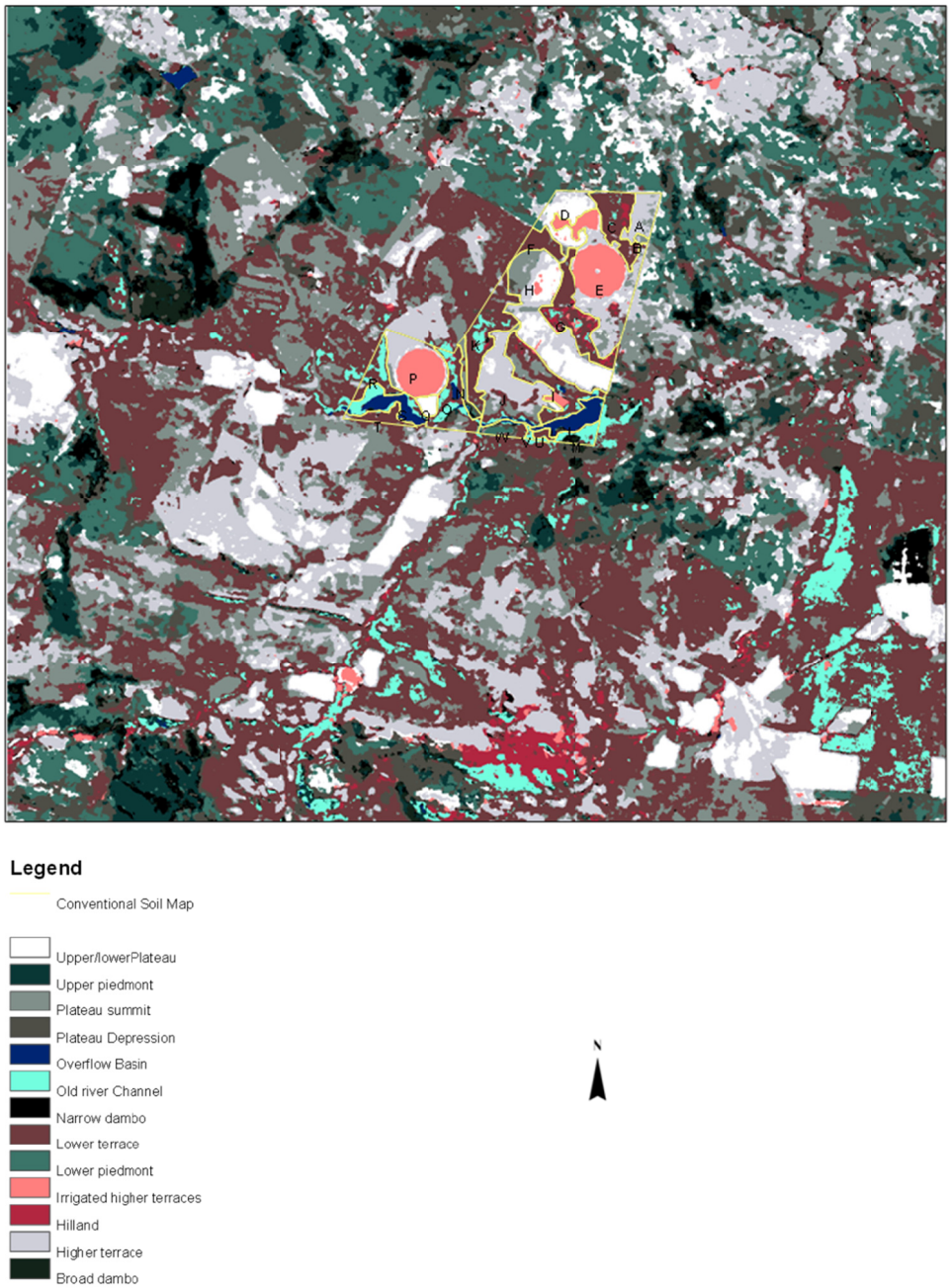

Figure 4. Conventional soil map covering part of the study area interfaced with Landsat-based soilscape map

Similarly, the Landsat derived map separated higher terraces from lower terraces as did the conventional soil survey map. Our soil profile descriptions showed that soil material deposited on the lower terrace near the stream had higher sand content and was better drained than that deposited on the higher terrace, further from the stream. Furthermore, the Landsat derived map separated at least three spectral classes, corresponding to three soil units, namely the plateau summit, higher terrace and upper/lower plateau with three soil classes (Typic Hapustults, Aquic Ustifluvents and Typic Paleustults) within polygon H (Figure 4). On the other hand, the conventional soil survey map indicates that this entire polygon consists of only one soil class, (Typic Rhodustults) as shown in Figure 3.

In the south east corner of the conventional soil survey map indicated as polygon M, the Landsat-based map showed that there are two mapping units, old river channel and broad dambo, that were classified as Vertic Endoaqualfs and Mollic Endoaqualfs, respectively. Both the false color composite, as well as our field

observation indicate that these are wet areas adjacent to the abandoned river channel. However, on the conventional soil map, this whole area was mapped as consisting of mollic Endoaqualfs.

The morphologically similar, but spectrally different higher terraces and irrigated higher terraces were both mapped as Aquic Ustifluvents on both the conventional soil survey map and the Landsat-based soil map.

In unit K of the conventional soil map the soil is classified as Aquic Ustifluvents, whereas on the Landsat-based soil map the unit consists of an association of two soil sub-groups (Vertic Endoaqualfs and Typic Ustifluvents). Map unit W which has more than one map units on the Landsat-based map was mapped as one unit on the conventional soil survey map. The area mapped I on the conventional soil map was classified as Typic Ustifluvents on both the conventional soil survey map as well as on the Landsat-derived soil map. However, field examination revealed no reason why the Landsat-derived map showed an additional unit of the plateau summit.

3.1 Classification Accuracy

Since the conventional soil map only covered a small portion of the study area, it could not be used to assess the classification accuracy for the whole classified image. For this reason accuracy assessment of the Landsat-based soil map was done by comparing the classified image with our field reference data. An overall classification accuracy of 72% was attained, meaning that 72% of the pixels from both the reference data and the classified image have the same classification category assigned to them. The overall Kappa Statistics obtained was 0.67. Accuracy assessment for the geomorphic soil units and the conditional Kappa for each category are presented in Table 5.

Table 5. Accuracy assessment for classification of soil units in the Chongwe region of Zambia

Geomorphic Unit	Dominant soil sub-group	Area (%)	Producer's accuracy (%)	User's accuracy (%)	Kappa
Hilland	Rhodic Haplustox	0.86	75	62	0.82
Upper Piedmont	Plinthic Haplustox	4.62	71	67	0.64
Lower Piedmont	Typic Paleustults	13.75	75	86	0.82
Plateau Summit	Typic Haplustults	15.47	77	88	0.85
Upper/Lower Plateau	Rhodic Haplustults	7.77	66	70	0.67
Plateau Depression	Typic Haplustepts	11.84	65	54	0.48
Higher Terrace	Aquic Ustifluvents	14.61	62	81	0.76
Higher Terrace-Irrigated	Acquic Ustifluvents	0.95	75	60	0.59
Lower Terrace	Typic Ustifluvents	23.84	61	59	0.52
Overflow Basin	Typic calciaquerts	0.33	54	39	0.58
Old River Channel	Vertic Endoaquafs	2.44	37	60	0.58
Narrow Dambos	Typic Fluaquents	0.99	50	20	0.19
Broad Dambos	Mollic Endoaqualfs	2.52	78	67	0.66

Note. Overall classification accuracy = 72%; Overall Kappa statistic = 0.67.

Overall, upland areas (hill-land, upper piedmont, lower piedmont plateau summit and upper/lower plateau) had the greatest accuracies when compared to ground observations. Most of these areas have characteristic features that make it easy to identify them as well as their spatial extent in the field.

The upper piedmont and lower piedmont have high spatial extents, making it somewhat easy to pick enough training pixels to define the spectral class characteristics. Plateau summits had the highest classification accuracy because they were very easy to identify in the field owing to the unique color of their surface soil (strong brown-7.5YR 5/8) derived from the color of termite mounds. The color of the surface soil in this unit made it spectrally different from other units, making it easy to find homogenous training pixels. This also applies to the upper/lower plateau areas whose surface soil color is also influenced by the color of the termite mounds (yellowish red-5YR4/6). However, the comparatively lower classification accuracy for this category can be attributed to colluvial deposits in this unit. Our field investigation revealed that colluvial sand deposition in this unit is still active. Generally, these sands occupy tracts of land adjacent to lower piedmont, plateau summit and

upper plateau soils. These sands of varying nature might have negatively affected the classification accuracy of this category. Sandier surface texture and brighter color in some parts of the unit may have caused this problem.

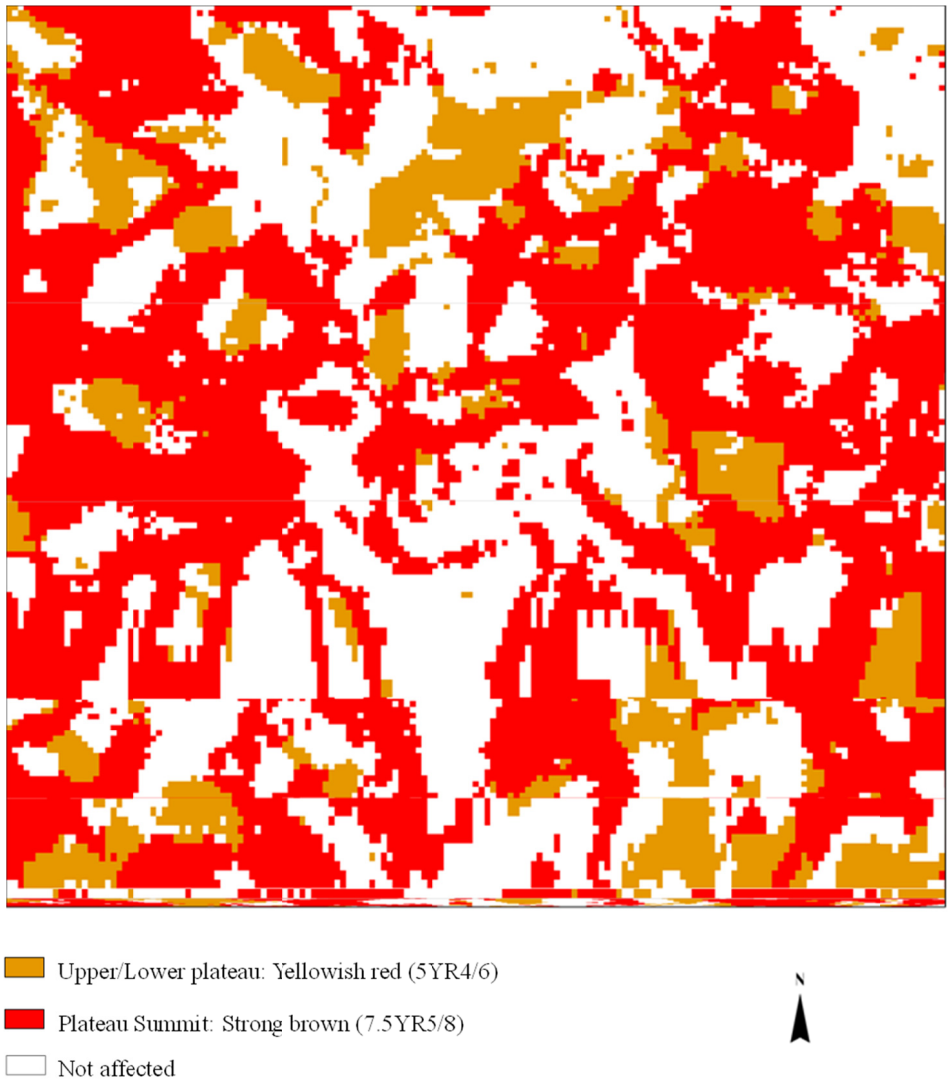

Figure 5. Parts of the study area in which soil color is influenced by the color of termite mounds

Lowland areas (lower terrace, overflow basin, old river channel, and narrow dambo) have the lowest classification accuracy. The lowest classification accuracy was found for the lower terrace.The error in this category may be due to the diverse origins of the alluvial sediments. Examination of field reference data indicates that there is considerable soil variability within this mapping unit. The soil material deposited near streams has a higher sand content and is well drained compared to the material deposited further away from the stream; however, the spectral characteristics could not be used to separate these two soil units.

The low classification accuracy for overflow basins and narrow dambos can be attributed to the small size of these areas. As seen from the Landsat-derived map (Figure 2) and from the classification accuracy assessment (Table 5), these two classes have very low spatial extent, making it difficult to obtain enough training pixels to adequately define the spectral class characteristics. The classification results for the old river channel (paleochannel) have low accuracy due to the coarse resolution of the Landsat data compared to spatial patterns of these geomorphic units. Field examination revealed that old river channels in the study area are not very broad; most of them are only 15-20 meters wide. Since this width is less than a Landsat ETM pixel (30 meter), the classifier algorithms may not have been well trained for this class.

Broad dambos had a higher classification accuracy compared to other lowland units. The most common clay mineral in these areas is smectite, which increases towards dambo centers making them susceptible to shrinkage on drying out. This leads to formation of wide cracks during periods of low rainfall. Field investigation showed that most of the grass was dead and dry in the central parts of the dambos, while towards the dambo margins the grass is greener, giving a darker toned rim to broad dambos. This made it easier to identify broad dambos both on the ground and on the Landsat imagery. They were imaged in very dark greenish brown color on the false color image with darker tones on the margins. The accuracies found by comparing point data to the Landsat-derived soil map are similar for what is found for comparison with traditional soil survey maps of comparable scales.

4. Conclusions

The study has shown that digital analysis of Landsat ETM data has the capability to delineate soilscape boundaries with reasonable accuracy. An overall classification accuracy of 72% was attained. Good agreement was found between Landsat data and field reference data, validating the hypothesis that spectral maps produced by digital analysis of Landsat ETM+ data compare favorably with field data. It is clear from the findings that upland soilscapes had higher classification accuracies compared to lowland soilscapes probably due to the diverse origin of sediments in the lowlands.

The study also demonstrated that Landsat data delineate soil boundaries similar to those in conventional soil maps. This means there is a strong relationship between spectral reflectance of soils and certain soil properties important to soil classification. Examining the spectral responses in different bands, it was found that spectral bands, 3, 5 and 7 provide images of optimum contrast for the delineation of soilscapes.

The role of termite mounds in influencing soil color and subsequently the spectral characteristics of the soil plays a significant role in delineating soilscapes in the Chongwe region of Zambia. Termite activities seem to be more prominent in upland soils, which is the main reason why soils on the plateau summit and the upper plateau were easily delineated in the field and classified with high accuracy on the Landsat image.

The study also revealed that the best time for acquiring soil information using Landsat data from natural landscapes in semi arid regions is in the dry season when there are long periods of cloud free skies, low soil moisture and minimal vegetation cover. The rainy season Landsat ETM data could not be easily related to soils because of vegetation cover. Therefore, Landsat ETM data from the rainy season is not reliable as a tool for soil mapping.

To demonstrate quantitatively that different mapping units and their soil sub-groups can be separated on the basis of spectral data, the mean relative reflectance values were plotted against their respective spectral bands. In most cases, the mean values were distinctly separable, indicating that soil sub-groups can be separated on the basis of spectral data.

Acknowledgements

This research work was conducted with funding support from the Inter-Disciplinary Center for the Study of Global Change (IGCC), Department of Forest Resources and Minnesota Agricultural Experiment Station, University of Minnesota. Logistical support received from the Ministry of Agriculture and Livestock is also acknowledged.

References

Brandt, R. T. (1958). *The geological structure of the upper Chalimbana area, East of Lusaka, Northern Rhodesia* (2nd ed.). Lusaka, Northern Rhodesia.

Buiten, H. J. (1993). Image interpretation: Visual or digital. *Current Topics in Remote Sensing, 3*, 507-513.

Chavez, P. S. Jr. (1989). Radiometric calibration of Landsat Thematic mapper multispectral images. *Photogrammetric Engineering and Remote Sensing, 55*, 1285-1294.

Chavez, P. S. Jr. (1996). Image-based atmospheric corrections—Revisited and revised. *Photogrammetric Engineering and Remote Sensing, 62*(9), 1025-1036.

Cipra, J. E., Franzmeier, D. P., Bauer, M. E., & Boyd, R. K. (1980). Comparison of multispectral measurements from some nonvegetated soils using Landsat digital data and a spectroradiometer. *Soil Science Society of America Journal, 44*(1), 80-84. http://dx.doi.org/10.2136/sssaj1980.03615995004400010018x

Cohen, W. B., & Goward, S. N. (2003). Landsat's role in ecological applications of remote sensing. *Bioscience, 54*(6), 535-545. http://dx.doi.org/10.1641/0006-3568(2004)054[0535:LRIEAO]2.0.CO;2

Dixey, F. (1955). Some aspects of geomorphology of Central and Southern Africa. *Geological Society of South Africa, 58*(2), 6-25.

Dozier, J., & Frew, J. (1981). Atmospheric corrections to satellite radiometric data over rugged terrain. *Remote Sensing of Environment, 11*, 191-205. http://dx.doi.org/10.1016/0034-4257(81)90019-5

Duggin, M. J., & Robinove, C. J. (1990). Assumptions implicit in remote sensing data aquisition and analysis. *International Journal of Remote Sensing, 11*(10), 1669-1694. http://dx.doi.org/10.1080/01431169008955124

Dwivedi, R. S., Singh, A. N., & Raju, K. K. (1981). Spectral reflectance of some typical Indian soils as affected by tillage and cover types. *Journal of the Indian Society of Remote Sensing, 9*(2), 33-40.

FAO. (1990). *Guidelines for soil profile description* (3rd ed.). Rome, Italy. Food and agriculture organization

Gerstl, S. A. W. (1990). Physics concepts of optical and radar reflectance signatures. *International Journal of Remote Sensing, 11*(7), 1109-1117. http://dx.doi.org/10.1080/01431169008955083

Kristof, S. J., & Zachary, A. L. (1971). Mapping soil types from Multispectral Scanner Data. *Remote Sensing of Environment, 3*, 2095-2108.

Mathews, H. L., Cunningham, R. L., Cipra, J. E., & West, T. R. (1973a). Application of Multispectral Remote Sensing to Soil Survey Research in Southeastern Pennsylvania. *Soil Science Society of America Journal, 37*(1), 88-93. http://dx.doi.org/10.2136/sssaj1973.03615995003700010029x

Moran, M. S., Ray, D. J., Philip, N. S., & Philippe, M. T. (1992). Evaluation of simplified procedures for retrieval of land surface reflectance factors from satellite sensor output. *Remote Sensing of Environment, 41*(2-3), 169-184. http://dx.doi.org/10.1016/0034-4257(92)90076-V

Otterman, J., & Fraser, R. S. (1976). Earth-atmosphere system and surface reflectivities in arid regions from Landsat MSS data. *Remote Sensing of Environment, 5*, 247-266. http://dx.doi.org/10.1016/0034-4257(76)90054-7

Piwowar, J. M., & LeDrew, E. F. (2002). ARMA time series modelling of remote sensing imagery: A new approach for climate change studies. *International Journal of Remote Sensing, 23*(24), 5225-48. http://dx.doi.org/10.1080/01431160110109552

Reddy, R. S., & Hilwig, F. W. (1993). Color additive viewing techniques for small scale soil mapping in an area of Karimnagar district, Andhra-Pradesh, India. *International Journal of Remote Sensing, 14*, 1705-1714. http://dx.doi.org/10.1080/01431169308953996

Shepande, C. (2010). *Development of geospatial analysis tools for inventory and mapping of soils of the Chongwe Region of Zambia* (Doctoral dissertation, University of Minnesota, St. Paul, USA).

Singh, S. M. (1988). Estimation of multiple reflection and lowest order adjacency effects on remotely sensed data. *International Journal of Remote Sensing, 9*, 1433-1450. http://dx.doi.org/10.1080/01431168808954951

Soil Survey Unit of the Department of Agriculture-Zambia. (1988). *Semi-detailed soil survey of Chongwe. 1:50000*. Chongwe, Zambia.

USDA. (2003). *Keys to Soil Taxonomy* (9th ed.). Washington DC: Government Printing Office.

Weismiller, R. A., Persinger, I. D., & Montgomery, O. L. (1977). Soil inventory from digital analysis of satellite scanner and topographic data. *Soil Science Society of America Journal, 41*(6), 1166-1170. http://dx.doi.org/10.2136/sssaj1977.03615995004100060031x

Weismiller, R. A., Persinger, I. D., & Montgomery, O. L. (1979). *Soil inventory prepared from digital analysis of satellite multispectral scanner data and digitized topographic data.* Laboratory for Applications of Remote Sensing, Purdue University, West Lafayette, Indiana.

Westin, F. C., & Frazee, C. J. (1976). Landsat data, its use in a soil survey program. *Soil Science Society of America Journal, 40*(1), 81-89. http://dx.doi.org/10.2136/sssaj1976.03615995004000010024x

Zachary, J. E., Cipra, R. I., Diderickson, S. J., Kristof, S. J., & Baumgardner, M. F. (1972). *Application of multispectral remote sensing to soil survey research in Indiana.* Agricultural Experiment Station, Purdue University, West Lafayette, Indiana.

Zidat, F. M., Taylor, J. C., & Brewer, T. R. (2003). Merging Landsat TM imagery with topographic data to aid soil mapping in the Badia region of Jordan. *Journal of Arid Environments, 54*, 527-541. http://dx.doi.org/10.1006/jare.2002.1076